Diffusion of magnetic fields into conductors of nonuniform resistivity

J. C. Sprott
Department of Physics, University of Wisconsin, Madison, Wisconsin 53706

(Received 4 August 1986; accepted for publication 7 October 1986)

Solutions are obtained for the spatial variation of electrical resistivity of cylindrical and rectangular conductors such that the magnetic field external to the conductor maintains a constant spatial variation as the magnetic field diffuses into the conductor. Practical implementations of the ideal solution are described.

I. INTRODUCTION

Sometimes it is desirable to produce or shape a magnetic field with a current-carrying conductor in such a way that the spatial variation of the magnetic field external to the conductor is constant as the magnetic field diffuses into the conductor. An example is a pulsed, magnetic device for plasma confinement. In such a case the stability and confinement properties are often determined by the shape of the magnetic field, and it is usually desired that the magnetic field remain tangent to the surface of the conductor so that there is no direct path for the plasma to escape by flowing parallel to the magnetic field into a material surface. Such considerations are especially important for devices with internal rings such as toroidal multipoles[1] and poloidal divertor tokamaks[2,3] as well as for devices with close-fitting conducting shells such as spheromaks[4,5] and reversed-field pinches.[6] An example as shown in Fig. 1 is a quadrupole magnetic field produced by currents in two, circular, resistive rods, and surrounded by a thick resistive wall which might be the vacuum vessel in which the plasma is confined.

In this paper we consider conductors of two prototypical shapes, a circular cylinder such as the resistive rod in Fig. 1 and a rectangular slab such as might be used to represent the resistive wall in Fig. 1. A resistivity variation is sought that will render the external magnetic field shape insensitive to diffusion. Practical implementations of the ideal resistivity variation are described. Conductors of more complicated shapes can be represented approximately by the solutions described.

The general equation which describes the diffusion of a magnetic field $\mathbf{B}$ into a conductor of nonuniform resistivity ρ is

$$\nabla^2\mathbf{B} - \frac{\nabla\rho}{\rho}\times(\nabla\times\mathbf{B}) = \frac{\mu_0}{\rho}\frac{\partial \mathbf{B}}{\partial t}. \quad (1)$$

The task is to find a spatial function ρ that will cause the direction, although not necessarily the magnitude, of the vector $\mathbf{B}$ to remain constant in time in the region external to the conductor. We will specialize to the case in which there is initially no magnetic field normal to the conductor surface, but we allow the tangential magnetic field to have a spatial dependence which we attempt to maintain as the magnetic field diffuses into the conductor. We will also assume that any currents external to the conductor which contribute to the field at its surface are fixed in space and have magnitudes proportional to the field at the surface of the conductor.

Rather than solve the full diffusion equation [Eq. (1)], we will solve for the resistive ($\partial \mathbf{B}/\partial t = 0$) limit and argue that a conductor that has the proper boundary conditions in the inductive ($t = 0$) and resistive ($t \rightarrow \infty$) limits will probably closely approximate the desired solution at intermediate times. As an added condition we can require that the variation of the resistivity at the surface be such that the boundary condition is satisfied asymptotically at early times ($t \rightarrow 0$) when the field has diffused only a small distance into the conductor. With this added condition, the resulting solution is, for all practical purposes, identical to the exact solution.

II. LONG CIRCULAR CYLINDER

Consider the case of a long, circular cylinder centered on $r = 0$ and carrying a current I in the z direction. If all other curents are sufficiently small or far away, the magnetic field in the region external to the conductor is in the θ direction with magnitude $B = \mu_0 I/2\pi r$ for all time. However, we will consider the case in which other nearby currents cause the field at the surface to deviate from perfect axisymmetry. An example would be one of the current-carrying rods of Fig. 1.

From $\mathbf{B} = \nabla\times\mathbf{A}$, we can define a flux function $\psi = -A_z$. From $\nabla\times\mathbf{B} = \mu_0\mathbf{j}$ and $\nabla\cdot\mathbf{A} = 0$ (Coulomb gauge), the current density is $\mathbf{j} = -\nabla^2\mathbf{A}/\mu_0$, or in cylindrical coordinates,

$$j_z = \frac{1}{\mu_0 r}\frac{\partial}{\partial r}\left(r\frac{\partial\psi}{\partial r}\right) + \frac{1}{\mu_0 r^2}\frac{\partial^2\psi}{\partial\theta^2}. \quad (2)$$

The magnetic field is

$$\mathbf{B} = -\frac{1}{r}\frac{\partial\psi}{\partial\theta}\hat{r} + \frac{\partial\psi}{\partial r}\hat{\theta}. \quad (3)$$

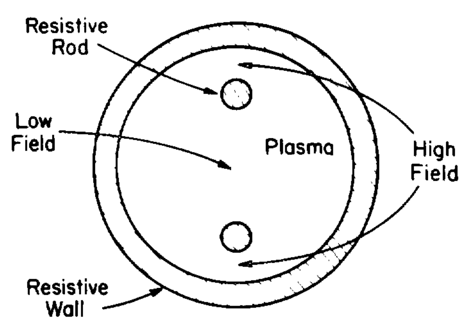

FIG. 1. Configuration in which a plasma is confined by the quadrupole magnetic field produced by electric currents in two resistive rods. The currents are into the page and return in a resistive wall which might also be the vacuum vessel.

 0021-8979/87/030817-05$02.40

Without loss of generality, we can define the flux to be zero at $r = 0$ and 1 at the surface of the conductor, which we take to have a dimensionless radius of $r = 1$. We consider only the lowest Fourier component of the field variation at the surface of the conductor and write the boundary conditions thus:

$$\psi(r=0) = 0, \tag{4}$$

$$\psi(r=1) = 1, \tag{5}$$

$$B_\theta(r=1) = \alpha(1 + \epsilon \sin\theta), \tag{6}$$

$$j_z(r=1) = \beta(1 + \epsilon \sin\theta)^2. \tag{7}$$

In the resistive limit, the electric field **E** is constant over the cross section of the cylinder, and the solution of the desired conductivity $\sigma(r,\theta)$ is the same as the solution of $j_z(r,\theta)$ since $\mathbf{j} = \sigma\mathbf{E}$. However, solutions in which j_z is not unidirectional are unphysical.

As stated above, the problem is underspecified, and a variety of solutions are possible. In order to proceed, we adopt the strategy of choosing a ψ function that is sufficiently simple to evaluate analytically and yet sufficiently complicated to allow the boundary conditions to be satisfied with one free parameter that can be varied to exhibit a range of possibilities. A function that meets these requirements is

$$\psi(r,\theta) = a(\theta)r + b(\theta)r^2 + c(\theta)r^3 + d(\theta)r^4. \tag{8}$$

From the boundary conditions and the requirement that j_z be finite and continuous at $r = 0$, the coefficients can be determined:

$$\begin{aligned}\psi = &-(\alpha\epsilon/2)r\sin\theta \\ &+ [3 - \alpha + d_0 - (\alpha\epsilon^2/2)\cos 2\theta]r^2 \\ &+ [\alpha - 2 - 2d_0 + (\alpha\epsilon/2)\sin\theta + \alpha\epsilon^2\cos 2\theta]r^3 \\ &+ [d_0 - (\alpha\epsilon^2/2)\cos 2\theta]r^4,\end{aligned} \tag{9}$$

where d_0 is a free parameter in terms of which α and β are given by

$$\alpha = \beta/2 = 2(3 - d_0)/(3 - \epsilon^2). \tag{10}$$

The form of Eq. (9) is such that $\psi(r=0) = 0$ and $\psi(r=1) = 1$, and the value of B_r derived therefrom becomes zero at $r = 1$ (as desired) while B_θ at $r = 1$ has the form shown by Eq. (6). From Eq. (2) we obtain

$$\begin{aligned}\mu_0 j_z = &\ 12 - 4\alpha + 4d_0 + (9\alpha - 18 - 18d_0 + 4\alpha\epsilon\sin\theta \\ &+ 5\alpha\epsilon^2\cos 2\theta)r + (16d_0 - 6\alpha\epsilon^2\cos 2\theta)r^2.\end{aligned} \tag{11}$$

The form of Eq. (11) is such that with α given by Eq. (10), $j_z(r=1)$ is of the relatively simple form proposed by Eq. (7) with $\beta = 2\alpha$. A useful parameter is the ratio of maximum to minimum value of B at the surface:

$$v = B_{\max}/B_{\min} = (1+\epsilon)/(1-\epsilon). \tag{12}$$

Contours of ψ and j_z (or σ) over the cross section of the cylinder for $v = 2$ for various values of d_0 are shown in Fig. 2. The solutions span the range from a low conductivity core surrounded by highly conducting shell ($d_0 < 0$) to a highly conducting core surrounded by a low conductivity shell ($d_0 > 0$).

Guided by the solutions above, we are led to consider practical implementations in which the cylinder is constructed of two different materials of conductivity σ_0 and σ_1

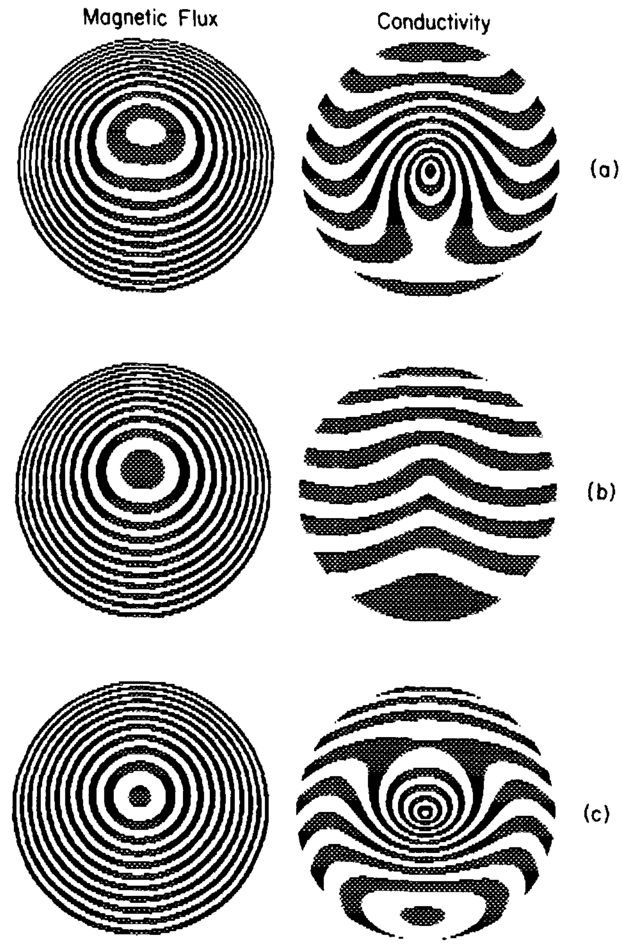

FIG. 2. Contours of magnetic flux and conductivity inside a cylinder for which the magnetic field on the surface varies by a factor of $v = 2$ in the resistive limit. The contours are normalized to a value of unity at the top of the figure and are in units of 0.1. (a) $d_0 = -0.5$, (b) $d_0 = 0$, (c) $d_0 = 0.5$.

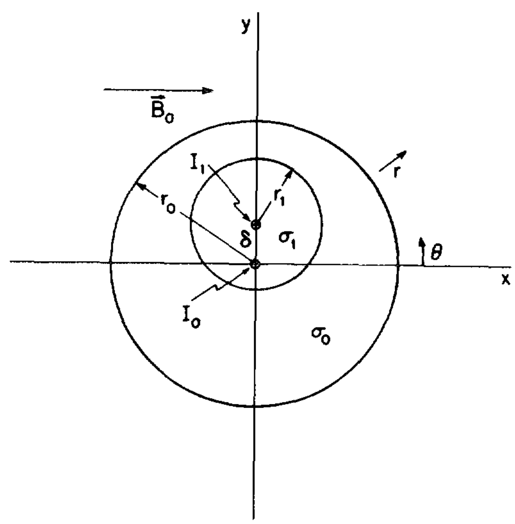

FIG. 3. Configuration in which a circular cylinder of conductivity σ_1 is embedded in a circular cylinder of conductivity σ_0 but with centers offset by an amount δ. In the resistive limit, the field external to the outer cylinder can be calculated as if filamentary currents were located on the axes of the cylinders.

with one material embedded in a circular cavity in the other but with a center offset from the axis by an amount δ as shown in Fig. 3. For such a configuration, the field at the surface can be calculated as a superposition of the field due to each of the cylinders and a field B_0 due to the external currents. In carrying out the calculation, the large cylinder is treated as if it were solid with a uniform conductivity σ_0, and the smaller cylinder is treated as if it had a conductivity $\sigma_1 - \sigma_0$ so as to cancel the contribution of the large cylinder over the region occupied by the smaller cylinder. In the resistive limit, the field due to the cylinders can be calculated as if the currents were concentrated in filaments on their axes. The field B_0 is taken as a constant over the surface as would be the case if the other currents are sufficiently far away.

The filamentary currents are given by

$$I_0 = \sigma_0 I/\sigma \tag{13}$$

and

$$I_1 = (\sigma - \sigma_0)I/\sigma, \tag{14}$$

where σ is the average conductivity,

$$\sigma = \sigma_0 + (\sigma_1 - \sigma_0)r_1^2/r_0^2. \tag{15}$$

From Eq. (12), B_0 can be calculated:

$$B_0 = \frac{v-1}{v+1}\frac{\mu_0 I_0}{2\pi r_0} + \frac{\mu_0 I_1}{2\pi(v+1)}\left(\frac{v}{r_0+\delta} - \frac{1}{r_0-\delta}\right). \tag{16}$$

If we require that the flux function ψ have the same value on the high-and low-field sides of the cylinder, we obtain the result:

$$B_0 = \frac{\mu_0 I_1}{4\pi r_0}\ln\left(\frac{r_0+\delta}{r_0-\delta}\right). \tag{17}$$

Equations (16) and (17) are a pair of simultaneous nonlinear equations which can be solved for δ and B_0. To lowest order in δ/r_0, the solutions are

$$\delta \cong \frac{r_0}{2}\frac{v-1}{v+1}\frac{\sigma}{\sigma-\sigma_0} \tag{18}$$

and

$$B_0 \cong \frac{\mu_0 I}{4\pi r_0}\frac{v-1}{v+1}. \tag{19}$$

In the region external to the cylinder, the flux per unit length is given by

$$\psi(x,y) = B_0 y + \frac{\mu_0 I_0}{4\pi}\ln(x^2+y^2) + \frac{\mu_0 I_1}{4\pi}\ln[x^2+(y-\delta)^2], \tag{20}$$

assuming B_0 is constant over the region considered.

Sample flux plots for the case of $v = 2$ and $r_1 = r_0/2$ with $\sigma_0 = 0$ and $\sigma_1 = 0$ are shown, respectively, in Figs. 4(a) and 4(b). These flux plots represent the resistive limit and have the feature that the flux is approximately tangent to the boundary as would be the case in the inductive limit as shown in Fig. 4(c) and are quite unlike the soaked-in, resistive limit of a cylinder with constant resistivity as shown in Fig. 4(d).

Although similar flux plots can be produced with the high conductivity material either on the inside or outside, the internal inductance is quite different in the two cases.

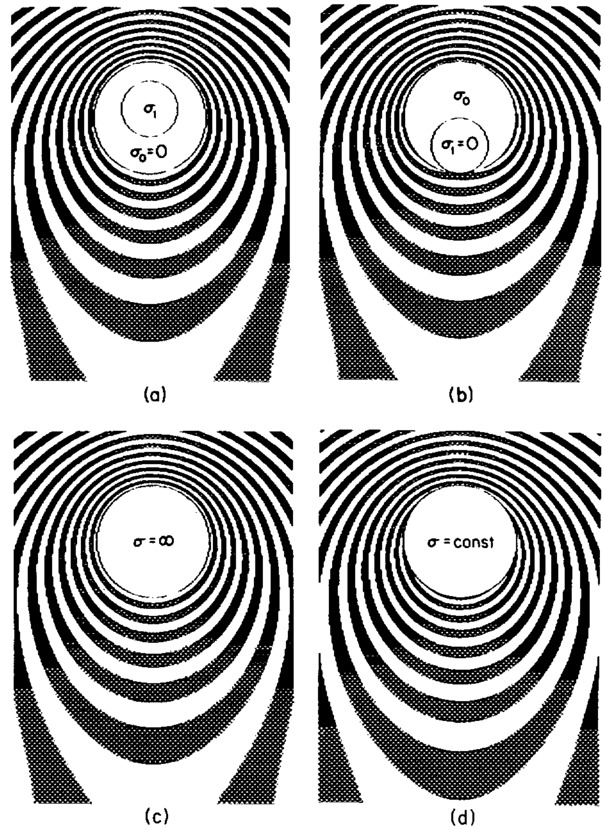

FIG. 4. Contours of magnetic flux in the region surrounding a cylinder for a magnetic field that varies by a factor of $v = 2$ on the surface. (a) high conductivity core, (b) high conductivity shell, (c) infinite conductivity, inductive limit, (d) uniform conductivity, resistive limit.

This difference may be important because it determines the magnetic energy that must be provided by the power supply as well as the flux swing that is required in a transformer-driven system. The inductance L can be calculated by equating $LI^2/2$ to the total magnetic energy inside the cylinder:

$$L = \frac{l}{\mu_0 I^2}\int_0^{r_0} B^2 2\pi r\, dr, \tag{21}$$

where l is the length of the cylinder. The general case is

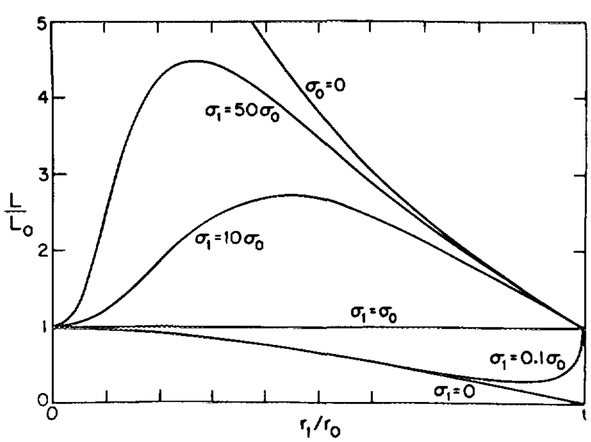

FIG. 5. Normalized internal inductance of a symmetrically layered cylinder for various conductivity ratios. The inductance is smallest when the high conductivity material is on the outside.

difficult to calculate, but a representative case is $\delta = 0$ (or $v = 1$) for which B is cylindrically symmetric and L is given by

$$L = \frac{\mu_0 l}{8\pi\sigma^2}\left[2(\sigma-\sigma_0)^2 \ln\left(\frac{\sigma_1-\sigma_0}{\sigma-\sigma_0}\right) + \sigma_0^2 + (\sigma_1^2 - \sigma_0^2) \times \frac{(\sigma-\sigma_0)^2}{(\sigma_1-\sigma_0)^2} + 4\sigma_0(\sigma-\sigma_0) - \frac{4(\sigma-\sigma_0)^2\sigma_0}{\sigma_1-\sigma_0}\right]. \tag{22}$$

The inductance, normalized to the internal inductance of a cylinder of constant resistivity ($\mu_0 l/8\pi$), is plotted in Fig. 5 versus r_1/r_0 for various ratios of σ_1/σ_0.

III. LARGE RECTANGULAR SLAB

Consider the case of a large, rectangular slab of thickness d in the x direction with a current density j_z in the z direction. The current is assumed to return in such a way that the magnetic field is entirely on the positive x side of the slab. This idealization would approximately represent the wall in Fig. 1 in the limit where the wall thickness is much less than the radius of curvature.

The current density inside the slab is given in terms of the flux function ψ by

$$j_z = \frac{1}{\mu_0}\left(\frac{\partial^2\psi}{\partial x^2} + \frac{\partial^2\psi}{\partial y^2}\right), \tag{23}$$

and the magnetic field is

$$\mathbf{B} = -\frac{\partial\psi}{\partial y}\hat{x} + \frac{\partial\psi}{\partial x}\hat{y}. \tag{24}$$

Without loss of generality, we can define the flux to be zero on the back side of the slab at $x = 0$ and 1 on the front surface of the slab which we take to have a dimensionless thickness of $d = 1$. We consider only the lowest Fourier component of the field variation at the surface of the conductor and write the boundary conditions thus:

$$\psi(x=0) = 0, \tag{25}$$

$$\psi(x=1) = 1, \tag{26}$$

$$B_y(x=1) = \alpha(1 + \epsilon \sin ky), \tag{27}$$

$$j_z(x=1) = \beta(1 + \epsilon \sin ky)^2. \tag{28}$$

In the resistive limit, the electric field $\mathbf{E}$ is constant over the cross section of the slab, and the solution of the desired conductivity $\sigma(x,y)$ is the same as the solution of $j_z(x,y)$ since $\mathbf{j} = \sigma\mathbf{E}$. However, solutions in which j_z is not unidirectional are unphysical.

As in the case with the cylinder, the problem is underspecified, and we choose a flux function

$$\psi(x,y) = a(y)x^2 + b(y)x^3 + c(y)x^4. \tag{29}$$

From the boundary conditions, the coefficients can be determined:

$$\psi = [3 + c_0 - \alpha - \alpha\epsilon \sin ky - (\alpha\epsilon^2/2)\cos 2ky]x^2 + (\alpha - 2 - 2c_0 + \alpha\epsilon \sin ky + \alpha\epsilon^2 \cos 2ky)x^3 + [c_0 - (\alpha\epsilon^2/2)\cos 2ky]x^4, \tag{30}$$

where c_0 is a free parameter in terms of which α and β are given by

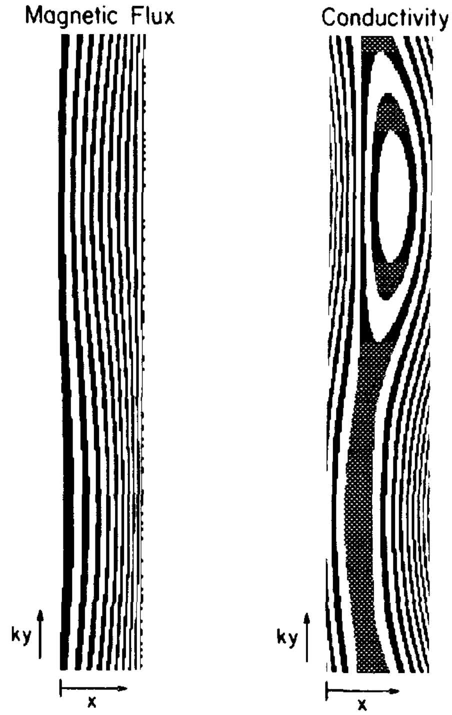

FIG. 6. Contours of magnetic flux and conductivity inside a slab for which the magnetic field on the surface varies by a factor of $v = 2$ in the resistive limit for $k = 0$ and $c_0 = 1$. The contours are normalized to a value of unity at the high field point on the right-hand surface and are in units of 0.1.

$$\alpha = \beta/2 = 2(3 - c_0)/(2 - \epsilon^2). \tag{31}$$

From Eq. (23) we obtain

$$\mu_0 j_z = 6 + 2c_0 - 2\alpha - 2\alpha\epsilon \sin ky - \alpha\epsilon^2 \cos 2ky + (6\alpha - 12 - 12c_0 + 6\alpha\epsilon \sin ky + 6\alpha\epsilon^2 \cos 2ky)x + [12c_0 - \alpha\epsilon^2(6 - 2k^2)\cos 2ky + \alpha\epsilon k^2 \sin ky]x^2 - \alpha\epsilon k^2(\sin ky + 4\epsilon \cos 2ky)x^3 + 2\alpha\epsilon^2 k^2 x^4 \cos 2ky. \tag{32}$$

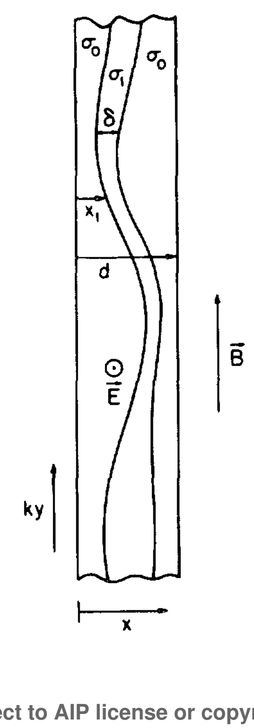

FIG. 7. Configuration in which a slab of conductivity σ_1 and width δ is embedded in a slab of conductivity σ_0 and width d.

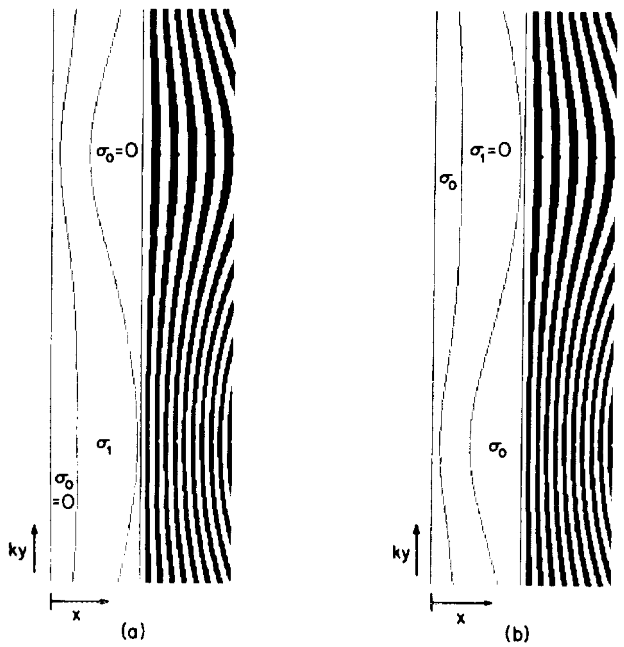

FIG. 8. Contours of magnetic flux in the region outside a slab of variable conductivity for a magnetic field that varies by a factor of $v = 2$ on the surface. (a) high conductivity interior with $\sigma = \sigma_1/2$ and $C = -\sigma_1 d^2/2$, (b) insulating interior with $\sigma = \sigma_0/2$ and $C = 3\sigma_0 d^2/2$.

Contours of ψ and j_z (or σ) over the cross section of the slab for $k = 0$ and $v = 2$ for a typical value of $c_0 = 1$ are shown in Fig. 6. This case has a low-conductivity band sandwiched in a high-conductivity material.

From the solution above, we are led to consider practical implementations in which a variable thickness layer of conductivity σ_1 is sandwiched between two layers of conductivity σ_0 as shown in Fig. 7. The quantities d, σ_0, and σ_1 are constant, and the quantities δ and x_1 are functions of y. In the resistive limit, the current j_z is produced by a constant electric field E in the z direction. By the principle of superposition, the magnetic field for the case of $kd \ll 1$ in the region $x > d$ is given by

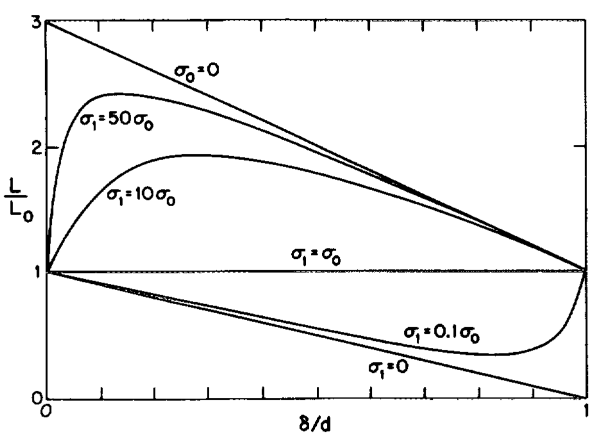

FIG. 9. Normalized internal inductance of a layered slab for various conductivity ratios. The inductance is smallest when the high conductivity material is on the side toward the magnetic field.

$$B = \mu_0\sigma_0 Ed + \mu_0(\sigma_1 - \sigma_0)E\delta. \tag{33}$$

Equating this field to the desired variation in Eq. (27) gives

$$\frac{\delta}{d} = \frac{\sigma(1 + \epsilon \sin ky) - \sigma_0}{\sigma_1 - \sigma_0}, \tag{34}$$

where σ is a free parameter which determines the average thickness δ for a given choice of σ_0 and σ_1. The quantity σ lies between σ_0 and σ_1 but is further constrained by the requirements $\delta > 0$ and $\delta + x_1 < d$.

From the requirement that the flux be constant at $x = d$ we are led to an equation for x_1 for the case of $kd \ll 1$:

$$x_1 = \frac{C - (\sigma_1 - \sigma_0)(\delta^2 - 2d\delta) - \sigma_0 d^2}{2\delta(\sigma_1 - \sigma_0)}, \tag{35}$$

where C is a free parameter that must be chosen to make $x_1 > 0$ and $x_1 + \delta < d$.

Sample flux plots for the case of $v = 2$ with $\sigma_0 = 0$ and $\sigma_1 = 0$ are shown, respectively, in Fig. 8. These flux plots represent the resistive limit and have the feature that the flux is tangent to the boundary as would be the case in the inductive limit. Identical flux plots can be obtained with a high conductivity material embedded within an insulator [Fig. 8(a)] and with an insulator embedded within a high conductivity material [Fig. 8(b)].

Although identical external flux plots can be produced with the high conductivity material either on the inside or outside, the internal inductance is quite different in the two cases. The general case is difficult to calculate, but a representative case is $\epsilon = 0$ and $x_1 = 0$ for which B is uniform in the y direction and L is given by

$$L = \frac{\mu_0 w}{l}\left(\frac{\sigma_1^2\delta^3}{3\sigma^2 d^2} + \frac{(\sigma - \sigma_0)^2(d - \delta)}{\sigma^2} + \frac{\sigma_0(\sigma - \sigma_0)(d^2 - \delta^2)}{\sigma^2 d} + \frac{\sigma_0^2(d^3 - \delta^3)}{3\sigma^2 d^2}\right), \tag{36}$$

where σ is an average conductivity given by

$$\sigma = \sigma_0 + (\sigma_1 - \sigma_0)\delta/d. \tag{37}$$

The inductance, normalized to the internal inductance of a slab of constant resistivity ($\mu_0 w/ld$), is plotted in Fig. 9 versus δ/d for various ratios of σ_1/σ_0.

ACKNOWLEDGMENTS

The author is grateful to Professor D. W. Kerst and Professor S. C. Prager for their useful comments and suggestions. This work was supported by the U. S. Department of Energy and the National Science Foundation.

[1] J. C. Sprott and S. C. Prager, Nucl. Fusion **25**, 1179 (1985).
[2] M. Keilhacker, Nucl. Fusion **25**, 1045 (1985).
[3] K. Bol, M. Okabayashi, and R. Fonck, Nucl. Fusion **25**, 1149 (1985).
[4] B. L. Wright, A. R. Sherwood, A. G. Sgro, D. A. Platts, J. Marshall, G. J. Marklin, R. K. Linford, S. O. Knox, P. L. Klingner, T. R. Jarboe, H. W. Hoida, I. Henins, J. C. Fernándes, and C. W. Barnes, Nucl. Fusion **25**, 1313 (1985).
[5] M. Yamada, Nucl. Fusion **25**, 1327 (1985).
[6] H. A. B. Bodin and A. A. Newton, Nucl. Fusion **20**, 1255 (1980).